Biosensors and Bioelectronics 101 (2018) 60–65

Contents lists available at ScienceDirect

Biosensors and Bioelectronics

journal homepage: www.elsevier.com/locate/bios

A novel three-dimensional carbonized $PANI_{1600}$@CNTs network for enhanced enzymatic biofuel cell

Zepeng Kang[a], Kailong Jiao[a], Jin Cheng[a], Ruiyun Peng[b], Shuqiang Jiao[a], Zongqian Hu[b,*]

[a] State Key Laboratory of Advanced Metallurgy, University of Science and Technology Beijing, Beijing 100083, PR China
[b] Beijing Institute of Radiation Medicine, Beijing 100850, PR China

ARTICLE INFO

Keywords:
3D carbon composite
Polyaniline
In situ polymerization
Biofuel cell

ABSTRACT

A novel three-dimensional (3D) carbon composite of $PANI_{1600}$@CNTs with rhizobium-like structure is prepared by in-situ polymerization of aniline monomers around and along the functionalized carbon nanotubes (CNTs) and then carbonized at 1600 °C for enzymatic biofuel cells (EBFCs). The SEM and TEM images clearly show that the carbonized PANI grew seamlessly on the surface of CNTs and presented the rhizobium-like structure. The carbonized PANI acts like conductive "glue" and connects the adjacent tubes together, which can assemble the CNTs into a 3D network. The $PANI_{1600}$@CNTs composite modified glassy carbon electrodes based on glucose oxidase (GOx) and laccase (Lac) exhibit high electrochemical performance. A glucose//O_2 EBFC constitutes of the fabricated anode and cathode performs a maximum power density of 1.12 mW cm^{-2} at 0.45 V. Furthermore, three of the fabricated EBFCs in series are able to lightening up a yellow light-emitting diode (LED) whose turn-on voltage is about at 1.8 V. This work may be helpful for exploiting novel substrates by carbonizing the composites of conducting polymer with nano materials at high-temperature for immobilization of enzymes in the EBFCs or biosensor fields.

1. Introduction

Enzymatic biofuel cells (EBFCs) is a type of fuel cell that utilizes enzymes as the electrocatalysts to catalyze the oxidation of fuel and/or the reduction of oxygen or peroxide to convert chemical energy into electricity (Rasmussen et al., 2016). However, EBFCs are limited by the relatively slow rate of electron transfer between enzyme and electrode, which is a major barrier for improving the power output (Chen et al., 2015b). Because the active centers of the redox enzymes are usually buried inside the protein matrices, establishing a reliable and efficient electrical contact between the biocatalyst and the electrode surface is the urgently required (Blaik et al., 2016; Prasad et al., 2014). A common approach of overcoming the electron transfer issue is by using a redox mediator molecule to facilitate electron transfer, namely the mediated electron transfer (MET) process (Blaik et al., 2016). However, the additional reagents, such as redox mediators, can be harmful to the biological activity of enzyme and reduce the open-circuit potential (OCP). The mediator-less electron transfer between biocatalysts and electrode surface is thus more favored (Navaee and Salimi, 2015).

GOx is one of the common oxidases in the application of bioanode towards glucose oxidation (Atanassov et al., 2007; Minteer et al., 2007). However, direct electrochemistry of GOx is still a big issue, while some researchers claimed the direct electron transfer (DET) process is possible and other groups insisted it is not. Due to the size of the protein (roughly 160 kDa) and the location of the FAD (deeply buried in the center of the protein), it is hard to believe DET can be occurred (Liang et al., 2015). Still, some researchers detected a quasi-reversible peak near −0.5 to −0.4 V (depending on pH and reference electrodes) at the GOx-modified electrodes and they claimed to obtain DET (Gao et al., 2014; Kowalewska and Jakubow, 2017; Liu et al., 2007).

Lac is a typical multicopper oxidase and has been intensively studied as biocathode electrocatalysts for oxygen reduction in biofuel cells by exploiting direct and mediated electron-transfer reactions (Barrière et al., 2006; Karnicka et al., 2008; Prasad et al., 2014; Zhang et al., 2014). However, achieving the DET system of Lac is still very hard due to the complicated catalytic mechanism and the strict enzyme molecular immobilized orientation (Matijošytė et al., 2008; Tominaga et al., 2015). Therefore, most studies are focused on mediated electron-transfer reaction for obtaining high effective electron transfer (Barrière et al., 2004; Zhang et al., 2014). Developing a new type electrode materials for immobilization of Lac and its mediators is the key step to construct the biocathode (Prasad et al., 2014).

In recent years, considerable efforts have been made to develop new materials as well as stable and efficient immobilization techniques for

* Corresponding author.
E-mail address: huzongqian@hotmail.com (Z. Hu).

http://dx.doi.org/10.1016/j.bios.2017.10.008
Received 1 September 2017; Received in revised form 30 September 2017; Accepted 2 October 2017
Available online 07 October 2017
0956-5663/

obtaining the DET of GOx and immobilizing the Lac and its mediators. For example, various conductive nanoparticles (Fang et al., 2016; Gutierrez-Sanchez et al., 2012; Huang et al., 2012) organic polymers (Crepaldi et al., 2014; Peng et al., 2013; Uk Lee et al., 2013) or carbon nanomaterials (Babadi et al., 2016; Gao et al., 2014) have been developed and used as an ideal conducting channel to promote efficient DET. Among the various conductive nanomaterials, carbon, with special morphology, high electrical conductivity, stable mechanical and thermal properties, plays an important role in the EBFCs fields (Chen et al., 2015b).

Carbonizing the nanostructured polymers, such as polyaniline (PANI) and polypyrrole (PPy), is a typical way to obtain various types of microporous carbon nanomaterials (Gavrilov et al., 2011; Janošević et al., 2012; Stejskal et al., 2010). In this work, we selected PANI as the carbon precursor, a novel 3D composite of PANI@CNTs with rhizobium-like structure were prepared by in-situ polymerization of aniline monomers along and around the surface of CNTs. The composite was carbonized at 1600 °C in accordance with our previous work (Kang et al., 2017). The carbonized composite of $PANI_{1600}$@CNTs was then used as the substrate for immobilization of GOx and Lac and their electrochemical properties were sufficiently studied.

2. Materials and methods

2.1. Synthesis of PANI and PANI@CNTs composite and carbonization

The PANI was synthesized by chemical oxidation polymerization of aniline monomers (Janošević et al., 2011). The detailed preparation processes of the PANI@CNTs composite were referenced to the previous reports (Ma et al., 2008; Zhou et al., 2010). Briefly, 200 mg of functional CNTs and 1.14 g of APS were suspended or dissolved in 80 mL of H_2SO_4 (1 M) solution, respectively, then put 373 mg of the aniline into the CNTs turbid liquid and sonicated for 30 min. After sonication, the mixture was stirred for 2 h by a magnetic stirring apparatus. Lastly, taking the APS solution into the mixture slowly under the condition of stirring. After that, the ultimate mixture was placed quietly for 24 h at the room temperature. The schematic diagram of the preparation procedures of PANI@CNTs composite was shown in Scheme 1. Carbonization was carried out through gradual heating (at 2 °C min^{-1}) to the target temperature 1600 °C at a nitrogen atmosphere and the product was denoted $PANI_{1600}$@CNTs.

2.2. Preparation of working electrode

For preparing the bioanode, a glassy carbon electrode (GCE) was sequentially polished using a slurry of 0.5 μm and 0.03 μm alumina power and successively washed by ultrasonication in deionized water, 1 M HNO_3, deionized water and ethanol for 3 min, respectively. Then the electrode was activated electrochemically in 0.1 M sulfuric acid by cyclic voltammetry (CV) until the CV curve to invariant (Inamuddin et al., 2014). Thereafter, the electrode was washed and dried in argon, then 6 μL of carbonized $PANI_{1600}$@CNT (5 mg mL^{-1}, prepared by deionized water) suspension was dropped on the surface of the cleaned GCE by using a microinjector, and then the electrode was dried in the air. The obtained electrode was denoted as $PANI_{1600}$@CNT/GCE. After that, 5 μL of GOx solution (4 mg mL^{-1}, prepared by PBS, pH 4) was spread onto the surface of $PANI_{1600}$@CNT/GCE electrode and then the electrode was left in a refrigerator (4 °C) for 6 h. The obtained electrode was denoted as GOx/$PANI_{1600}$@CNT/GCE. Finally, 4 μL of Nafion solution (1 *v/v*%, prepared by ethyl alcohol, 99.99%) was spread onto the surface of GOx/$PANI_{1600}$@CNT/GCE. Then left it in a refrigerator (4 °C) for 2 h. The final electrode was denoted as Nafion/GOx/$PANI_{1600}$@CNT/GCE. For comparison, Nafion/GC, Nafion/GOx/GC, Nafion/$PANI_{1600}$/GC, Nafion/GOx/CNTs/GC and Nafion/$PANI_{1600}$@CNT/GC electrodes were prepared through the same procedures as above.

The biocathode was fabricated as follows. Briefly, 6 μL of 5 mg mL^{-1} $PANI_{1600}$@CNT suspension was cast on the surface of an GCE, air-dried, followed by successive casting 4 μL of 10 mg mL^{-1} Lac solution (prepared by PBS, pH 4.0), and 3 μL of Nafion solution, and each casting was done after the previous cast had been air-dried. The as-prepared enzyme electrode was denoted as Nafion/Lac/$PANI_{1600}$@CNT/GCE. All the prepared enzyme electrodes were stored in PBS at 4 °C when not in use.

2.3. Electrochemical testing and BFC performance

All electrochemical experiments were carried out in an electrochemical workstation (CHI 660 C, CHI Instrument, Shanghai, China). The conventional three-electrode comprised a working electrode of modified glassy carbon (3 mm diameter), counter electrode of Pt (surface area: 1 cm^2), and reference electrode of Ag/AgCl (3 M KCl). The electrochemical measurements of bioanode were carried out in 0.1 M sodium phosphate buffer solution (PBS, pH 7.2), which was purged with high-purity argon for at least 30 min prior to experiments. An argon environment was kept over the solution in the cell. The electrochemical measurements of biocathode were carried out in 0.1 M Britton-Robison (B-R, pH 5.0) with or without 0.5 mM ABTS for oxidation of the oxygen. All experiments were performed at ambient temperature.

The glucose//O_2 EBFC was fabricated in two-compartments using acrylic glass and the anodic and cathodic compartments were separated by the Nafion 211 membrane. The Nafion/GOx/$PANI_{1600}$@CNT/GCE and the Nafion/Lac/$PANI_{1600}$@CNT/GCE were acted as the bioanode and the biocathode, respectively. The electrolyte of anodic compartment was the Ar-saturated 0.1 M PBS (pH 5.0) with 0.1 M glucose. The cathodic compartment was filled by the 0.2 M B-R buffer (pH 5.0) with 0.5 mM ABTS and continuously bubbled with the oxygen. The measurements of power density were referenced to previous report (Liu et al., 2012).

3. Results and discussion

3.1. Microscopic and spectroscopic characterization

Fig. 1 shows the SEM and TEM images of the (A, D) CNTs, (B, E) PANI@CNTs and (C, F) $PANI_{1600}$@CNTs composites. As can be seen in the Fig. 1**A** and **D**, the CNTs presented the typical nanotube structure and smooth surface. In Fig. 1**B,** it can be clearly seen that the surface of the graphite-structure CNTs was covered by a compact original PANI layer with a diameter of 60–80 nm. Fig. 1**E** shows the corresponding images of TEM, the PANI@CNTs composite exhibited a well-defined boundary and presented a core-shell structure. Obviously, the conducting polymer of PANI played a role of “glue” and connected the adjacent tubes together, which could make the CNTs into a three-dimensional network. Fig. 1**C** shows that the presence of nanotubes with a smaller diameter compared with that in the PANI@CNTs composite, which might be caused by the gases emission, such as CO, CO_2, CH_4, etc., during the calcination process. The amplified image (inset) exhibits a three-dimensional network of coadjacent nanotubes. Fig. 1**F** shows that the carbonized PANI distributed uniformly on the surface of CNTs and presented the rhizobium-like shape. The rhizobium-like carbon grew seamlessly on the surface of the CNTs and connected the adjacent tubes together, which could effectively reduce the resistance at the intertube junctions in the $PANI_{1600}$@CNTs network. All these results indicated that the $PANI_{1600}$@CNTs composite could be an excellent materials for immobilization of enzymes in the application of biofuel cells or biosensors.

Fig. S1 shows the FT-IR spectra of (curve a) original CNTs, (curve b) functional CNTs, (curve c) aniline-CNTs and (curve d) PANI@CNTs. The stretching bands at 1620 cm^{-1} and 1380 cm^{-1} are the vibration of C = C and C–H (curve a). The increased stretching band for C = O at

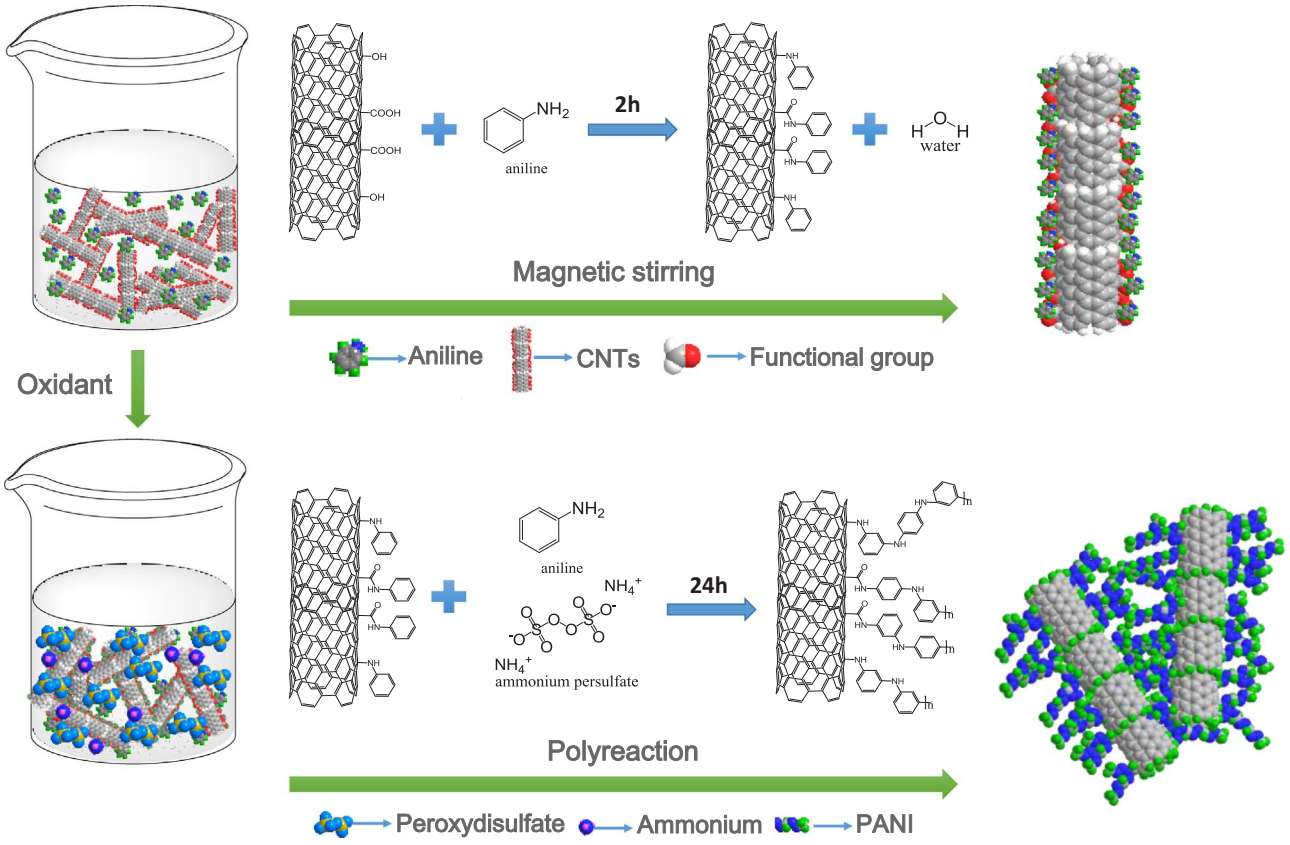

Scheme 1. Schematic diagram for the preparation of the PANI@CNTs composite.

1750 cm^{-1} is assigned to the carboxyl groups, indicating the functionalized CNTs was successfully obtained (curve b) (Zhang et al., 2014). In the FT-IR spectrum of aniline-CNTs (curve c), the peaks at 1420 cm^{-1} and 1240 cm^{-1} are ascribed to the stretching vibration of C = N and N - H from the amide groups (Li et al., 2015), indicating that the aniline monomers were successfully covalent bonded on the surface of CNTs. Two striking differences among the four spectra in the curve d are found in –N = quinoid = N– stretching at 1490 cm^{-1} and

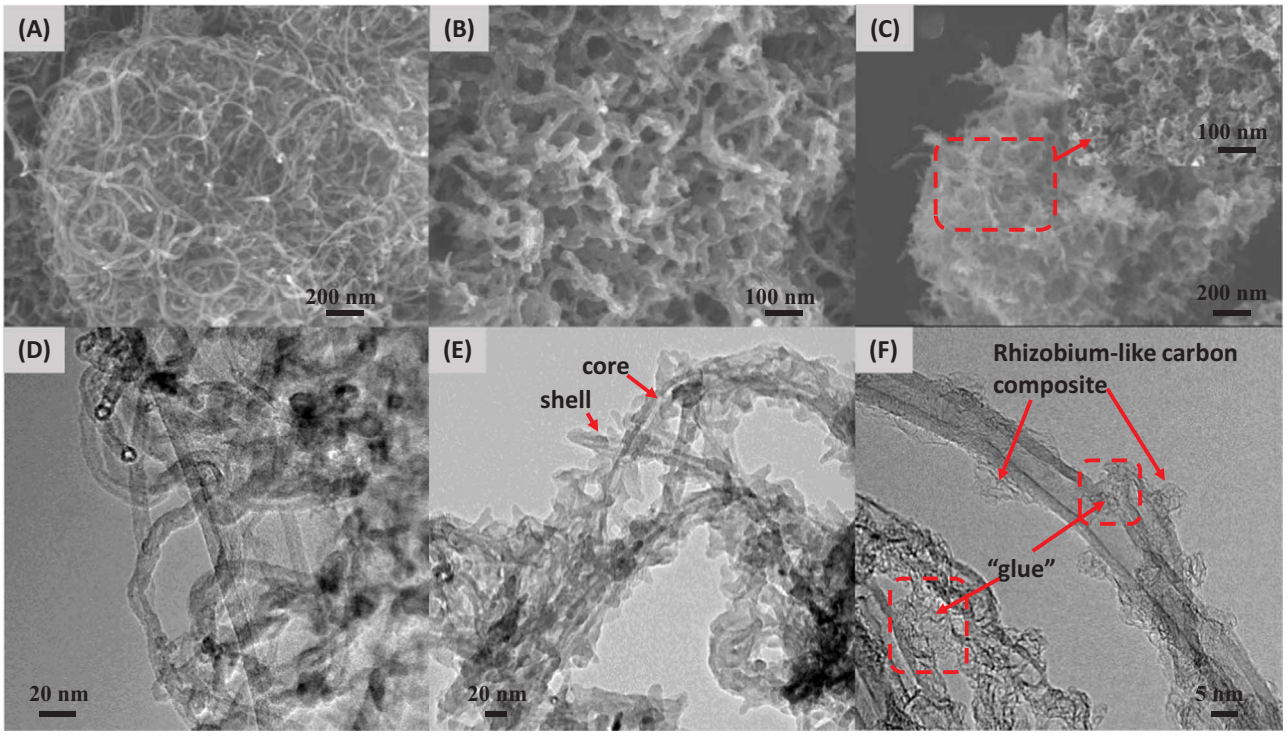

Fig. 1. SEM images of (A)CNTs, (B) PANI@CNTs and (C) $PANI_{1600}$@CNTs composite ; TEM images of (D)CNTs, (E) PANI@CNTs and (F) $PANI_{1600}$@CNTs composite.

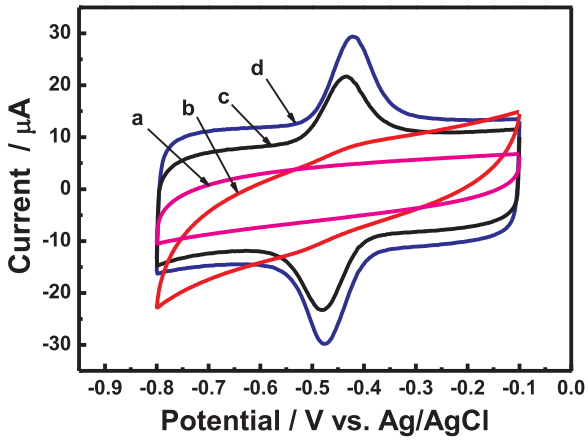

Fig. 2. CVs of (a) Nafion/$PANI_{1600}$@CNTs/GCE, (b) Nafion/GOx/CNTs/GCE, (c) Nafion/GOx/$PANI_{1600}$/GCE, (d) Nafion/GOx/$PANI_{1600}$@CNTs/GCE electrodes. All experiments were conducted in 0.1 M pH 7.2 PBS at a scan rate of 50 mV s^{-1}.

1120 cm^{-1}, which were attributed to the typical structure of PANI (Ma et al., 2008). These results suggesting that the PANI@CNTs composite with a core-shell structure was successfully synthesized by in situ polymerization.

3.2. Direct electrochemical properties of bioanode

Fig. 2 shows the CVs of the (a) Nafion/$PANI_{1600}$@CNTs/GCE, (b) Nafion/GOx/CNTs/GCE, (c) Nafion/GOx/$PANI_{1600}$/GCE, and (d) Nafion/GOx/$PANI_{1600}$@CNTs/GCE in 0.1 M argon-saturated PBS (pH 7.2) at a scan rate of 50 mV s^{-1}. Obviously, no redox peak was observed in curve **a**, whereas a pair of weaken redox peak presented in curve **b**. In addition, a pair of well-defined redox peak was displayed in both curve **c** and **d**, with the formal potential $E^{'0}$ was estimated to be −0.454 V and −0.451 V, respectively. These values were very close to the previous reported redox peaks of GOx for its cofactor $FAD/FADH_2$ (Gao et al., 2014), indicating that the direct electron transfer of GOx was achieved by the $PANI_{1600}$ and $PANI_{1600}$@CNTs. As for the peak current of curve **d** was larger than that of curve **c**, it might be attributed to the 3D network of $PANI_{1600}$@CNTs which could enhance the active loading of GOx. Furthermore, the peak potential separation ($\triangle E_P$) of curve **d** was 48 mV and smaller than 54 mV of curve **d**, indicating a faster electron transfer.

The pH value of the supporting electrolyte will influence the direct electron transfer of GOx (Gao et al., 2014). Fig. 3**A** shows the CVs of Nafion/GOx/$PANI_{1600}$@CNTs/GCE electrode in different pH values of PBS solution at a scan rate of 50 mV s^{-1}. Both the anodic and cathodic peak potentials shifted to negative direction with the increase of the electrolyte pH. The formal potential exhibited a linear dependence on the pH ranging from 5 to 9 with a slope of −60.6 mV/pH (R^2 = 0.998) (Inset), which is very close to the theoretical value of −59.2 mV/pH (Liang et al., 2015), indicating that two protons participated in the electron transfer process (Gao et al., 2014; Hyun et al., 2015a).

In order to evaluate the electron transfer, the CVs of the Nafion/GOx/$PANI_{1600}$@CNTs/GCE electrode were investigated at different scan rates. As can be seen from Fig. 3**B**, the redox peak currents clearly increased with increasing potential scan rate. Moreover, the anodic peak currents (I_{Pa}) and reduction peak current (I_{Pc}) were proportional to the scan rate v (inset a), and the liner regression equations are expressed as I_{Pa} (μA) = 0.191 v (mV s^{-1}) + 9.090 (R^2 = 0.995) and I_{Pc} (μA) = −0.196 v (mV s^{-1}) −9.640 (R^2 =0.995), suggesting a quasi-reversible surface-controlled electrochemical process (Li et al., 2015). Furthermore, the peak potential was linear with the Napierian logarithm of scan rates (at high scan rate, inset b), which was consistent to previous reports (Hyun et al., 2015b). According to Eq. (S1) and (S2) (Campbell et al., 2015), the α and n were calculated to be 0.32 and 1.83, respectively. Additionally, the k_s of the system was estimated to be 12.93 at 100 mV s^{-1} by equation S3 (Laviron, 1974), which was larger than that of the previous reports (Liu et al., 2007; Prasad et al., 2014). Based on Faraday's law $Q = nFA\Gamma^*$ (Campbell et al., 2015), where A is the effective surface area of the working electrode and Γ^* is the surface coverage of GOx, the Γ^* was calculated to be 6.24 × 10^{-8} mol cm^{-2}. This loading is almost 2 orders of magnitude higher than similar nanometer materials as previous reported (Peng et al., 2013; Zhang et al., 2014).

3.3. The electrocatalytic property of biocathode

Fig. 4**A** shows the CVs of Nafion/Lac/$PANI_{1600}$@CNTs/GCE in (a) Ar-saturated B-R buffer (0.1 M, pH 5), (b) O_2-saturated B-R buffer (0.1 M, pH 5), (c) Ar-saturated B-R buffer containing 0.5 mM ABTS (0.1 M, pH 5), (d) O_2-saturated B-R buffer containing 0.5 mM ABTS (0.1 M, pH 5). Obviously, no variations were observed on the curves **a** and **b**, indicating that the Nafion/Lac/$PANI_{1600}$@CNTs/GCE shows low catalytic activity toward oxygen reduction. This phenomenon can further illustrate that the DET didn't happen between the active center of Lac and the electrode. In fact, the DET requires a short distance (less than 15–20 Å) which is not straightforward in many cases (Tominaga et al., 2015; Zhang et al., 2014). A pair of well-defined redox peak was displayed in the curve **c**, which is the typical electracatalytic characteristic of ABTS (Karnicka et al., 2008). As shown in the curve **d**, a much larger cathodic current can be observed and the bioelectrocatalytic reduction of oxygen starts at 0.64 V which is higher than previous reports (Tan et al., 2009; Zhang et al., 2014). The observed

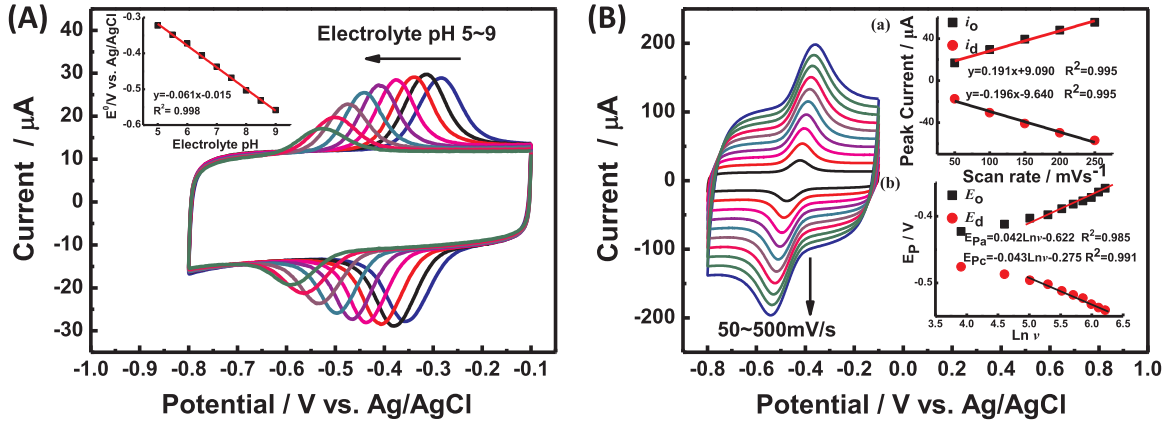

Fig. 3. (A) CVs of Nafion/GOx/$PANI_{1600}$@CNTs/GCE in 0.1 M Ar-saturated PBS (pH 7.2) at different pH values (from right to left): 5–9. Inset: $E^{'0}$ vs. pH. Scan rate: 50 mV s^{-1}; (B) CVs of Nafion/GOx/$PANI_{1600}$@CNTs/GCE in 0.1 M Ar-saturated PBS (pH 7.2) at different scan rate values (from inner to outer): 50–500 mV s^{-1}. Inset (a): I_p vs. v. Inset (b): E_p vs. log v.

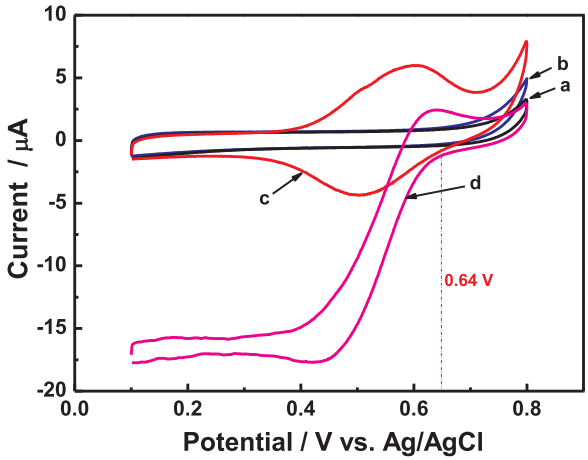

Fig. 4. CVs of Nafion/Lac/$PANI_{1600}$@CNTs/GCE in (a) Ar-saturated B-R buffer (0.1 M, pH 5), (b) O_2-saturated B-R buffer (0.1 M, pH 5), (c) Ar-saturated B-R buffer containing 0.5 mM ABTS (0.1 M, pH 5), (d) O_2-saturated B-R buffer containing 0.5 mM ABTS(0.1 M, pH 5); scan rate: 10 mV s^{-1}.

reduction currents increase rapidly during negative potential scanning, suggesting that the ABTS is an efficient electron transfer mediator which facilitate the electron transfer from the active center of Lac to the electrode surface. These results highlight the advantage of the fabricated Lac-based electrode for bioelectrocatalytic reduction of oxygen with the aid of ABTS.

3.4. Biosensor for glucose and biofuel cell

Fig. 5**A** shows the CVs of Nafion/GOx/$PANI_{1600}$@CNTs/GCE in air-saturated PBS with different concentrations of glucose at a scan rate of 50 mV s^{-1}. When the glucose was added, both the anode and cathodic currents decreased gradually with the increasing of glucose concentration (inset b). And the cathodic current was linear against the glucose concentration ranging from 0.07 to 0.88 mM with a sensitivity of 14.77 μA mM^{-1}. The calibration curve corresponding to cyclic voltammetry response was shown in inset a. The detection limit was estimated to be about 0.05 mM based on the criterion of a signal-to-noise ratio of 3 (Chen et al., 2015a). This phenomenon demonstrated that the immobilized GOx maintained its biocatalytic activity.

The performance of the assembled glucose//O_2 EBFC was further investigated under the optimum conditions. Fig. 5**B** displays the typical polarization curve and power output curve (*I*-V and *I*-P curves) of the EBFC at the room temperature (25 °C). The OCP and the short-circuit current were 0.78 V and 6.2 mA cm^{-2}, respectively. A maximum power density of 1.12 mW cm^{-2} was obtained at 0.45 V, which was superior to those previous reports on modified electrodes by using PANI or CNTs (Agnès et al., 2013; Fu et al., 2016; Zhang et al., 2012). The storage stability of the assembled bioelectrode kept at 4 °C was examined by recording power density of the EBFC by once a day (inset). After a period of two weeks, the power density measured were 0.928 mW cm^{-2}, which were ~ 82.85% lower than the corresponding initial values. Fig. 5**C** shows the pictures of the real anode, cathode and the assembled EBFCs. The OCP of three EBFCs in series was higher to 2.32 V and they were able to lighten up a yellow LED whose turn-on voltage is ~ 1.8 V. The operating voltage was maintaining at ~ 2.0 V. These results may be attributed to the 3D network structure of carbonized $PANI_{1600}$@CNTs, suggesting that $PANI_{1600}$@CNTs is a good platform for EBFCs.

4. Conclusions

In summary, a novel carbon composite of $PANI_{1600}$@CNTs with rhizobium-like structure was prepared. An exciting performance

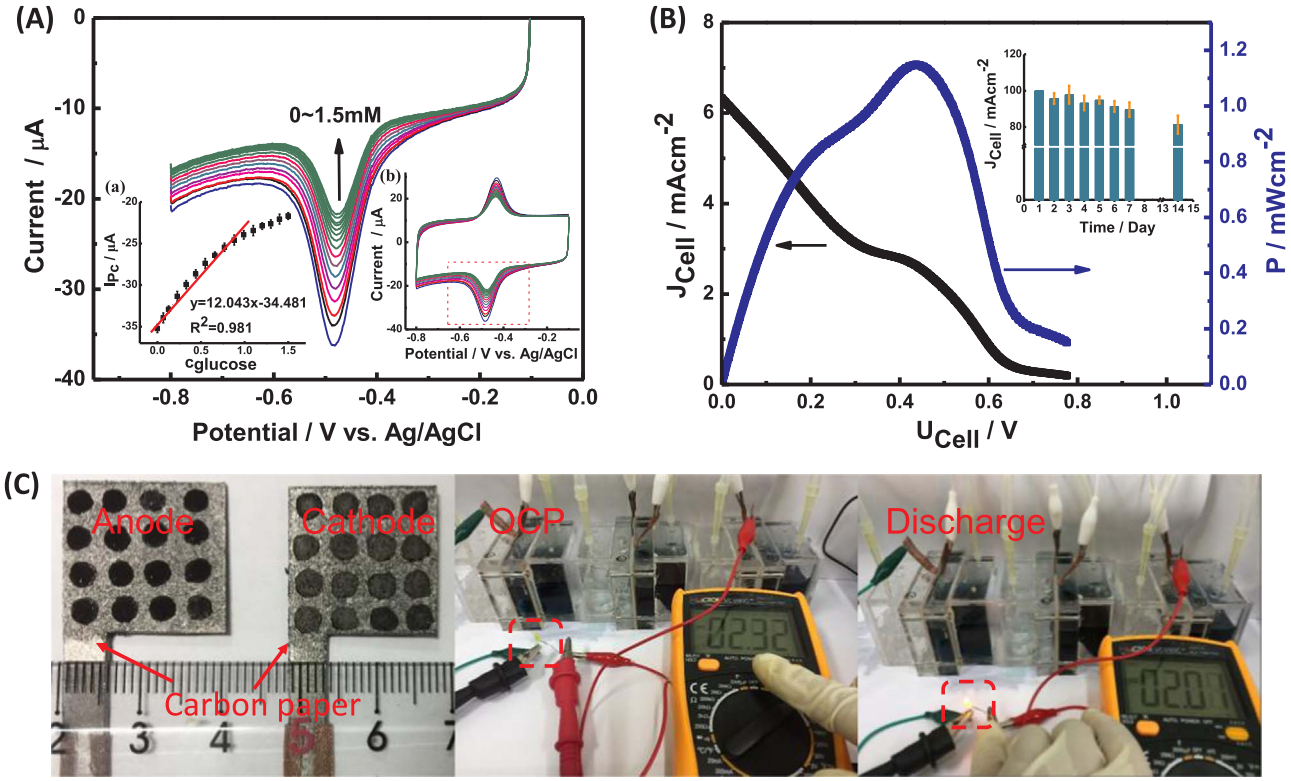

Fig. 5. (A) Half CVs of Nafion/GOx/$PANI_{1600}$@CNTs/GCE electrode in the air-saturated PBS (0.1 M, pH 7.2) solution with various concentrations of glucose, scan rate: 50 mV s^{-1}. Inset a: full CVs, inset b: the calibration curve of the linear dependence of cathodic peak current on the glucose concentration; (B)The power output characteristics of the prepared glucose biofuel cell obtained by LSV at 20 mV s^{-1}. Inset: Stability test of the biofuel cell (GOx, glucose//Pt/C, O_2). The value of power density control (100%) corresponds to 1.12 mW cm^{-2}. (C) A yellow LED powered by three EBFCs in series.

bioanode and biocathode have been yielded based on the carbonized $PANI_{1600}$@CNTs. The Nafion/GOx/$PANI_{1600}$@CNTs/GCE electrode not only showed efficient DET property, but also ideal catalytic activity towards glucose oxidation. The Nafion/Lac/$PANI_{1600}$@CNTs/GCE electrode exhibited efficient catalytic reduction of O_2 in the presence of ABTS. A glucose//O_2 EBFC consisting of the fabricated bioanode and biocathode outputted a maximum power density of 1.12 mW cm^{-2} at 0.45 V. In addition, three of the assembled EBFCs were able to lighten up a yellow LED whose turn-on voltage is ~ 1.8 V. These results proved that the carbonized $PANI_{1600}$@CNTs composite with well-defined rhizobium-like structure provided an excellent conductive 3D network for effective charge transfer, which provided better access to the electrode material for enzyme immobilization. Hence, carbonizing conducting polymers or their composites with inorganic materials at high temperature may be helpful to promote the practical application of EBFCs and also useful for the development of biosensors.

Acknowledgments

Financial support for this work was provided by National Natural Science Foundation of China through grant 81301345.

Notes and references

The authors declare no competing financial interest.

Appendix A. Supporting information

Supplementary data associated with this article can be found in the online version at http://dx.doi.org/10.1016/j.bios.2017.10.008.

References

Agnès, C., Reuillard, B., Le Goff, A., Holzinger, M., Cosnier, S., 2013. Electrochem. Commun. 34, 105–108.
Atanassov, P., Apblett, C., Banta, S., Brozik, S., Barton, S.C., Cooney, M., Liaw, B.Y., Mukerjee, S., Minteer, S.D., 2007. Interface-Electrochem. Soc. 16 (2), 28–31.
Babadi, A.A., Bagheri, S., Hamid, S.B., 2016. Biosens. Bioelectron. 79, 850–860.
Barrière, F., Ferry, Y., Rochefort, D., Leech, D., 2004. Electrochem. Commun. 6 (3), 237–241.
Barrière, F., Kavanagh, P., Leech, D., 2006. Electrochim. Acta 51 (24), 5187–5192.
Blaik, R.A., Lan, E., Huang, Y., Dunn, B., 2016. ACS Nano 10 (1), 324–332.
Campbell, A.S., Jeong, Y.J., Geier, S.M., Koepsel, R.R., Russell, A.J., Islam, M.F., 2015. ACS Appl. Mater. Interfaces 7 (7), 4056–4065.
Chen, J., Zhu, R., Huang, J., Zhang, M., Liu, H., Sun, M., Wang, L., Song, Y., 2015a. Analyst 140 (16), 5578–5584.
Chen, Y., Gai, P., Zhang, J., Zhu, J.-J., 2015b. J. Mater. Chem. A 3 (21), 11511–11516.
Crepaldi, L.B., Neto, S.A., Cardoso, F.P., Ciancaglini, P., De Andrade, A.R., 2014. Electrochim. Acta 136, 52–58.
Fang, L., Liu, B., Liu, L., Li, Y., Huang, K., Zhang, Q., 2016. Sens. Actuators B 222, 1096–1102.
Fu, Y.B., Liu, Z.H., Su, G., Zai, X.R., Ying, M., Yu, J., 2016. Fuel Cells 16 (3), 377–383.
Gao, Y.F., Yang, T., Yang, X.L., Zhang, Y.S., Xiao, B.L., Hong, J., Sheibani, N., Ghourchian, H., Hong, T., Moosavi-Movahedi, A.A., 2014. Biosens. Bioelectron. 60, 30–34.
Gavrilov, N., Vujković, M., Pašti, I.A., irić-Marjanović, G., Mentus, S.V., 2011. Electrochim. Acta 56 (25), 9197–9202.
Gutierrez-Sanchez, C., Pita, M., Vaz-Dominguez, C., Shleev, S., De Lacey, A.L., 2012. J. Am. Chem. Soc. 134 (41), 17212–17220.
Huang, Y., Qin, X., Li, Z., Fu, Y., Qin, C., Wu, F., Su, Z., Ma, M., Xie, Q., Yao, S., Hu, J., 2012. Biosens. Bioelectron. 31 (1), 357–362.
Hyun, K., Han, S.W., Koh, W.-G., Kwon, Y., 2015a. Int. J. Hydrogen Energy 40 (5), 2199–2206.
Hyun, K.H., Han, S.W., Koh, W.-G., Kwon, Y., 2015b. J. Power Sources 286, 197–203.
Inamuddin, Ahmad, K., Naushad, M., 2014. Int. J. Hydrogen Energy 39 (14), 7417–7421.
Janošević, A., Pašti, I., Gavrilov, N., Mentus, S., irić-Marjanović, G., Krstić, J., Stejskal, J., 2011. Synth. Met. 161 (19–20), 2179–2184.
Janošević, A., Pašti, I., Gavrilov, N., Mentus, S., Krstić, J., Mitrić, M., Travas-Sejdic, J., Ćirić-Marjanović, G., 2012. Microporous Mesoporous Mater. 152, 50–57.
Kang, Z., Jiao, K., Xu, X., Peng, R., Jiao, S., Hu, Z., 2017. Biosens. Bioelectron. 96, 367.
Karnicka, K., Miecznikowski, K., Kowalewska, B., Skunik, M., Opallo, M., Rogalski, J., Schuhmann, W., Kulesza, P.J., Chem, A., 2008. Anal. Chem. 80 (19), 7643–7648.
Kowalewska, B., Jakubow, K., 2017. Sens. Actuators B 238, 852–861.
Laviron, E., 1974. J. Electroanal. Chem. Interfacial Electrochem. 52 (3), 395–402.
Li, Z., Xie, C., Wang, J., Meng, A., Zhang, F., 2015. Sens. Actuators B 208, 505–511.
Liang, B., Guo, X., Fang, L., Hu, Y., Yang, G., Zhu, Q., Wei, J., Ye, X., 2015. Electrochem. Commun. 50, 1–5.
Liu, J., Zhang, X., Pang, H., Liu, B., Zou, Q., Chen, J., 2012. Biosens. Bioelectron. 31 (1), 170–175.
Liu, Q., Lu, X., Li, J., Yao, X., Li, J., 2007. Biosens. Bioelectron. 22 (12), 3203–3209.
Ma, Y., Cheung, W., Wei, D., Bogozi, A., Chiu, P.L., Wang, L., Pontoriero, F., Mendelsohn, R., He, H., 2008. ACS Nano 2 (6), 1197–1204.
Matijošytė, I., Arends, I.W.C.E., Sheldon, R.A., Vries, S.D., 2008. Inorg. Chim. Acta 361 (4), 1202–1206.
Minteer, S.D., Liaw, B.Y., Cooney, M.J., 2007. Curr. Opin. Biotechnol. 18 (3), 228–234.
Navaee, A., Salimi, A., 2015. J. Mater. Chem. A 3 (14), 7623–7630.
Peng, H.P., Liang, R.P., Zhang, L., Qiu, J.D., 2013. Biosens. Bioelectron. 42, 293–299.
Prasad, K.P., Chen, Y., Chen, P., 2014. ACS Appl. Mater. Interfaces 6 (5), 3387–3393.
Rasmussen, M., Abdellaoui, S., Minteer, S.D., 2016. Biosens. Bioelectron. 76, 91–102.
Stejskal, J., Trchová, M., Hromádková, Ji, Kovářová, J., Kalendová, A., 2010. Polym. Int. 59 (7), 875–878.
Tan, Y., Deng, W., Ge, B., Xie, Q., Huang, J., Yao, S., 2009. Biosens. Bioelectron. 24 (7), 2225–2231.
Tominaga, M., Sasaki, A., Togami, M., 2015. Anal. Chem. 87 (10), 5417–5421.
Uk Lee, H., Young Yoo, H., Lkhagvasuren, T., Seok Song, Y., Park, C., Kim, J., Wook Kim, S., 2013. Biosens. Bioelectron. 42, 342–348.
Zhang, J., Zhu, Y., Chen, C., Yang, X., Li, C., 2012. Particuology 10 (4), 450–455.
Zhang, Y., Chu, M., Yang, L., Tan, Y., Deng, W., Ma, M., Su, X., Xie, Q., 2014. ACS Appl. Mater. Interfaces 6 (15), 12808–12814.
Zhou, Y., Qin, Z.-Y., Li, L., Zhang, Y., Wei, Y.-L., Wang, L.-F., Zhu, M.-F., 2010. Electrochim. Acta 55 (12), 3904–3908.